

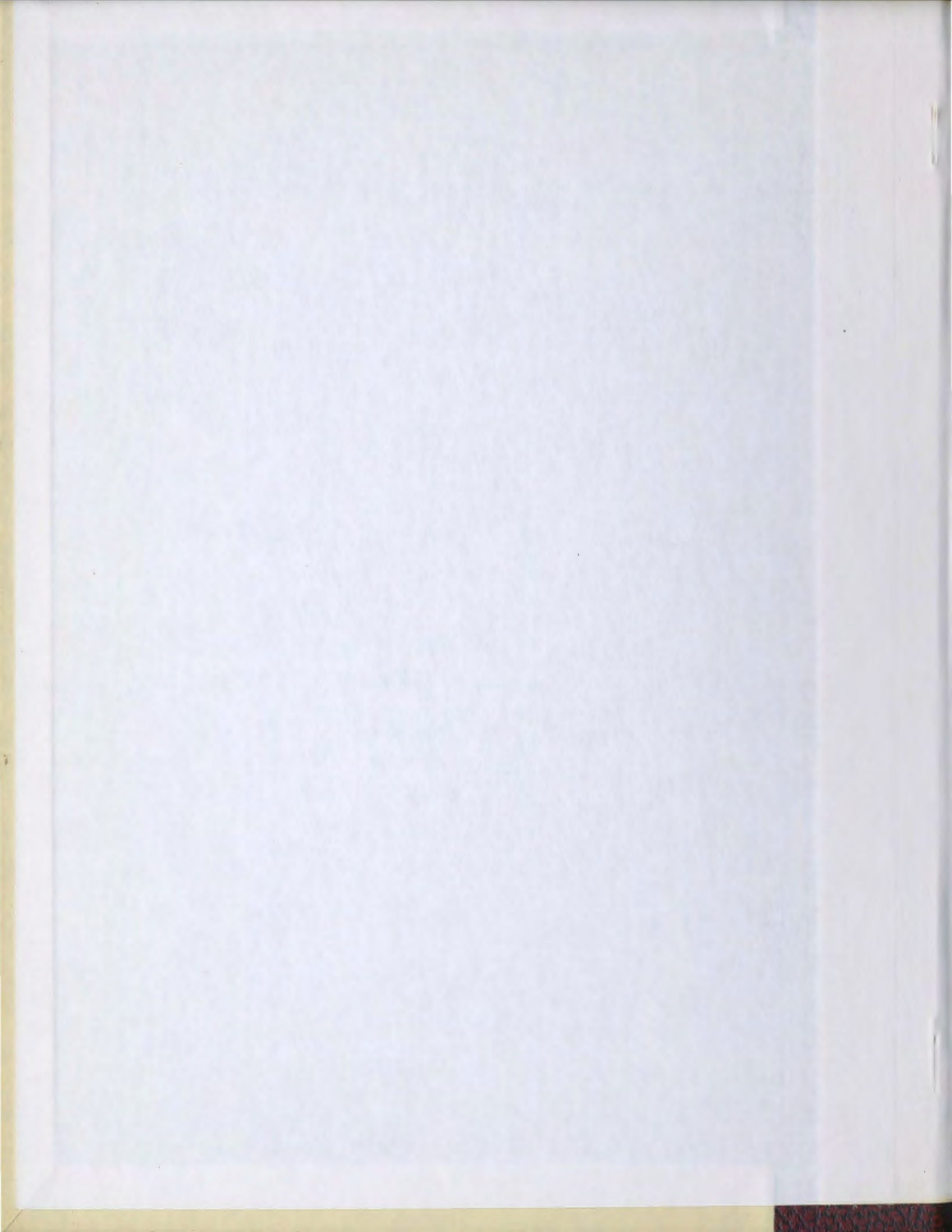
GAIN MEASUREMENTS IN 3, 3'DIETHYLTHIATRICARBOCYANINE IODIDE  
AS A FUNCTION OF PUMP POWER, WAVELENGTH, AND TIME

**CENTRE FOR NEWFOUNDLAND STUDIES**

**TOTAL OF 10 PAGES ONLY  
MAY BE XEROXED**

**(Without Author's Permission)**

PAUL G. GILLARD



354737





GAIN MEASUREMENTS IN 3,3'DIETHYLTHIATRICARBOCYANINE IODIDE  
AS A FUNCTION OF PUMP POWER, WAVELENGTH, AND TIME

by



Paul G. Gillard, B.Sc.

Submitted in partial fulfilment  
of the requirements for the degree of Master of Science,  
Memorial University of Newfoundland

March 27, 1973

ABSTRACT

The single-pass gain of a  $4 \times 10^{-5}$  M/l solution of 3.3' diethylthiatricarbocyanine iodide in methanol optically pumped by a giant pulse ruby laser was measured as a function of pump power, wavelength, and time. Pump power was varied over a range of 0 - 7 MW and the wavelength range was  $7850 \text{ \AA} - 8075 \text{ \AA}$ . The gain is seen to have very little dependence on time or the total energy in the pulse, but has strong dependence on the instantaneous pump power. The dependence of gain on pump power is plotted from the experimental data for six wavelengths in the region investigated, and is also discussed theoretically. The spontaneous decay rate from the excited state and the cross section for stimulated emission are also obtained from the theory. The low signal gain coefficient and the gain saturation value are tabulated for each wavelength investigated.

CONTENTS

ABSTRACT	i
CONTENTS	ii
LIST OF TABLES	iii
LIST OF FIGURES	iv
CHAPTER 1 Introduction	1
Dye lasers	2
CHAPTER 2 Experimental Apparatus and Procedures	7
A. Experimental arrangement	7
Ruby laser system	7
Dye laser oscillator	9
B. Gain measurement	14
Reduction of data	16
Absolute power calibration of photodiode PA	19
Temporal corrections	23
CHAPTER 3 Results and discussion	24
Analysis of data	24
Gain as a function of time	25
Gain as a function of instantaneous pump power	27
Gain as a function of wavelength	37
CHAPTER 4 Conclusion	39
REFERENCES	40
APPENDIX	41
ACKNOWLEDGEMENTS	44

LIST OF TABLES

TABLE I	Dyes which showed laser action and their spectral ranges	12
TABLE II	Observed gain and attenuation constants for DTTC dye in methanol at various wavelengths, with the transition probabilities and cross sections for these wavelengths	35

LIST OF FIGURES

Figure 1	8
Experimental setup used for gain measurement	
Figure 2	10
Dye laser oscillator	
Figure 3	13
Spectrograms of broadband dye laser output for the dyes	
(i) 3,3' diethylthiatricarbocyanine	
(ii) cryptocyanine	
(iii) 1,1' diethyl-2,2' thiadicarbocyanine iodide	
Figure 4	15
Tuned laser spectra for DTTC dissolved in methanol ( $10^{-5}$ moles/liter)	
Figure 5	18
Relative photodiode calibration	
Figure 6	20
Normalized input and output pulses for each of the six wavelengths used in the gain experiment	
Figure 7	22
Absolute power calibration of photodiode PA of Figure 1	
Figure 8	26
(a),(b) Gain as a function of pulse time	
(c),(d) Profiles of the pump pulse and the input and output pulses to the amplifier cell	

Figures 9(a) through 9(f)

28-33

Gain versus instantaneous pump power for six dye  
laser wavelengths

Figure 10

36

Gain versus wavelength for constant instantaneous  
pump power

CHAPTER 1

INTRODUCTION

In 1958 Schawlow and Townes (1) published the first papers suggesting the possibility of light amplification by stimulated emission, or laser action as it is now known. Stimulated emission compares with the absorption of light by a molecule in its ground state in that it is dependent on the number of molecules in the state and on the intensity of the incident light. For absorption, the number of molecules absorbing light per unit time  $N_{abs}$  is  $N_{abs} = N_g B_{ge} I$  where  $N_g$  is the ground state population,  $I$  is the incident light intensity, and  $B_{ge}$  is the transition probability per unit time for absorption. For stimulated emission, the number of molecules producing stimulated emission per unit time is  $N_{stim} = N_e B_{eg} I$  where  $N_e$  is the number of molecules in the excited state and  $B_{eg}$  is the transition probability per unit time for stimulated emission.

The other process by which light is emitted from the excited molecule is by spontaneous emission. Spontaneous emission depends only on the number of molecules in the excited state and the transition probability for the process. For spontaneous emission, the number of molecules per unit time spontaneously decaying to the ground state  $N_{spon}$  is  $N_{spon} = N_e A_{eg}$  where  $A_{eg}$  is the transition probability per unit time for spontaneous emission.

It can be shown that  $B_{eg} = B_{ge}$  and that  $\frac{A_{eg}}{B_{eg}} = \frac{8\pi h}{\lambda^3}$ . When  $N_e$  is greater than  $N_g$ , the population is said to be in population inversion.

This is inversion in comparison with the condition at thermal equilibrium when the states are populated according to the Boltzmann distribution. When a system has an inverted population and light is incident on the system, more light will be produced by stimulated emission than is absorbed, thereby producing a net gain or amplification of the incident light.

Schawlow and Townes (1) considered optical cavities consisting of two plane parallel reflecting surfaces which would reflect light back and forth through a medium which had an inverted population. They found the minimum population inversion required to support such a system to be

$$\Delta n = N_e - N_g = \frac{4\pi^2 \Delta\lambda_0}{\lambda_0^4} \frac{\tau_{eg}}{\tau_c} \quad [1]$$

where  $\tau_{eg}$  is the lifetime of the laser transition,  $\lambda_0$  is the central wavelength of the laser transition,  $\Delta\lambda_0$  is the linewidth of the laser transition, and  $\tau_c$  is the cavity lifetime, or the time required for light reflecting back and forth inside the empty cavity to reach  $\frac{1}{e}$  of its initial value.

$$\tau_c = \frac{n\ell}{(1-R)c}$$

where  $n$  is the index of refraction for the cavity,  $\ell$  is the separation between the end mirrors,  $R$  is the geometrical mean of the reflectivities ( $R = \sqrt{R_1 R_2}$ ), and  $c$  is the speed of light. For  $\ell = 10$  cm,  $n = 1$ , and  $R = 0.7$ , we get  $\tau_c \approx 1$  ns.

### Dye Lasers

A number of brightly luminescent organic compounds were possible candidates for laser action for several reasons: (i) Their ease in preparation, compared with crystalline materials, for example, (ii) their

optical homogeneity in solution, which reduces light loss due to scattering in the medium, and (iii) for many of these compounds the phosphorescent and fluorescent lifetimes were well known and, by choosing different substances, wide ranges of lifetimes were available. Early experiments with such compounds failed to achieve laser action, however, for reasons which will later become apparent.

In 1961 Brock et al (2) and Rautian and Sobelman (3) made the first theoretical considerations of organic dye laser action. They suggested the use of phosphorescence from the metastable triplet state of organic dye molecules. Attempts to achieve laser action along these lines failed, however, for the following reasons: (i) There are usually strongly allowed transitions to a higher triplet state which, because of the width of the laser line, often overlap the laser wavelength and seriously deplete the laser transition. (ii) Because of the long lifetime of the triplet state ( $\sim 10^{-5}$  sec) large excited state populations are required ( $10^{18} - 10^{23}/\text{cm}^3$ ), in which case non-radiative depopulation of the triplet state is quite complete. Also, at such concentrations, the dye solution would normally be virtually opaque and quite difficult to pump optically (4). For lasers based on fluorescent systems, however, since the ratio of fluorescent lifetimes to phosphorescent lifetimes is  $\sim 10^{-3}$ , the excited state populations necessary for inversion reduce by a factor of  $10^{-3}$ . From equation [1] we see that for a laser material with fluorescent lifetime  $10^{-9}$  sec and cavity lifetime  $10^{-9}$  sec and a bandwidth of  $100 \text{ \AA}$  at  $8000 \text{ \AA}$ , all of which can be realized physically with little difficulty, the population inversion is  $\approx 10^{12}/\text{cm}^3$ .

In 1963 Lempicki and Samuelson (5) reported the first organic dye laser system, using an alcohol solution of europium benzoylacetate. Other such metallo-organic compounds were also found to exhibit laser action, but these laser systems did not become competitive with gas or solid state laser systems, despite many improvements such as room temperature operation and extended wavelength ranges. This was mainly due to the high absorption coefficients of these compounds which limited the depth of penetration of the flashlamp light to only a few microns. For this reason, these materials have a higher threshold and lower conversion efficiency than solid state lasers.

In 1966 the first optically pumped organic dye laser system was developed by Sorokin and Lankard (4). Their laser material was a dilute solution of chloro-aluminum phthalocyanine which was optically pumped by a giant pulse ruby laser. They also made theoretical calculations concerning this system, and the effects they predicted were observed experimentally.

Since 1966, various dye solutions were found which would lase from the near ultraviolet to beyond  $1 \mu$  in the infrared, using flashlamps as well as various pulsed lasers as pumping sources. One group of dyes in particular, the polymethine group, includes dyes which can continuously cover the wavelength region from  $0.7$  to  $1.0 \mu$  when pumped by a giant pulse ruby laser, with output of the dye laser between 1 and 10 MW for a pumping power of 100 MW (6).

In 1967 Soffer and McFarland (7) used a plane reflecting grating set in autocollimation for one of the dye laser cavity reflectors, and achieved spectral narrowing of several orders of magnitude, from

100 Å to  $\approx 1$  Å with no apparent loss in output energy. Since this time, many ingenious methods have evolved for the efficient tuning of dye lasers; for example, Bradley et al (8) studied the effect of a Fabry-Perot interferometer inside a cavity which had an echelle grating as one of its reflectors. With this combination, spectral narrowing of  $10^4$  was achieved at a cost of output power decreasing by a factor of  $\frac{1}{4}$ .

In order to design efficient dye lasers and dye laser amplifiers, it is necessary to know the gain of the dye as a function of the parameters which can be varied. This gain can be calculated from theory or measured experimentally. However, in order to calculate the gain from theory, certain properties of the molecule in question must be known, such as fluorescent decay times from the excited states, non-radiative lifetime of the state, absorption cross sections for the ground state, and the rate of intersystem crossing between the excited singlet and excited triplet state. In the molecules which we study, these values are not all known. Therefore, the gains can be measured accurately only by experimental methods. From the gains measured experimentally, it may then be possible to evaluate, or at least place upper bounds on, some of the lifetimes. Gain measurements can also be related to the population inversion in the system in question.

Huth, in 1970 (9), measured the single-pass gain of a flashlamp pumped dye laser amplifier as a function of wavelength and time, for the dye Rhodamine 6 G in ethanol. Shank et al, using a different method from Huth's made gain measurements for this and other dyes in the visible region, and his results agreed with Huth's to within about 5%. Shank's experiment measured the gain of the dyes as a function of pump energy and wavelength.

This present work studies the gain of the dye 3,3'-diethylthiatricarbocyanine iodide (DTTC) in methanol, which exhibits laser action over the wavelength range of 7800 - 8400 Å, as a function of pump power, wavelength, and time.

## CHAPTER 2

### EXPERIMENTAL APPARATUS AND PROCEDURES

#### A. Experimental arrangement:

The setup used for this experiment is shown in Fig. 1. It consists of three principal parts; (i) a ruby laser oscillator, (ii) an organic dye laser oscillator, and (iii) an organic dye laser amplifier.

#### Ruby laser system:

The ruby laser system was a Korad model K1-Q, employing a 4" long and 9/16" in diameter ruby rod with 0.05% CrO<sub>3</sub>, which was pumped by a helical xenon flashlamp. The laser head which houses the rod and the flashlamp was cooled and held at a preset temperature by a Lauda-Brinkman water circulator, model K-2/R, capable of a  $\pm 0.10^{\circ}\text{C}$  temperature control.

Giant pulse operation of the laser system was obtained by using a bleachable dye, cryptocyanine, dissolved in methanol, which acted as a Q-switch. By proper choice of the electrical energy delivered to the flashlamp, and the concentration of the Q-switching dye solution, single pulses with greater than 100 MW peak powers and temporal halfwidths at half intensity of approximately 10 ns were obtained.

The Q-switching dye was contained in an Eastman cell #6097 consisting of two optically flat quartz plates, each 3/8" thick and 1-7/8" in diameter, separated by a 1.65 mm teflon spacer. Outside surfaces of the cell were antireflection coated to minimize reflection losses at 6943 Å wavelength.

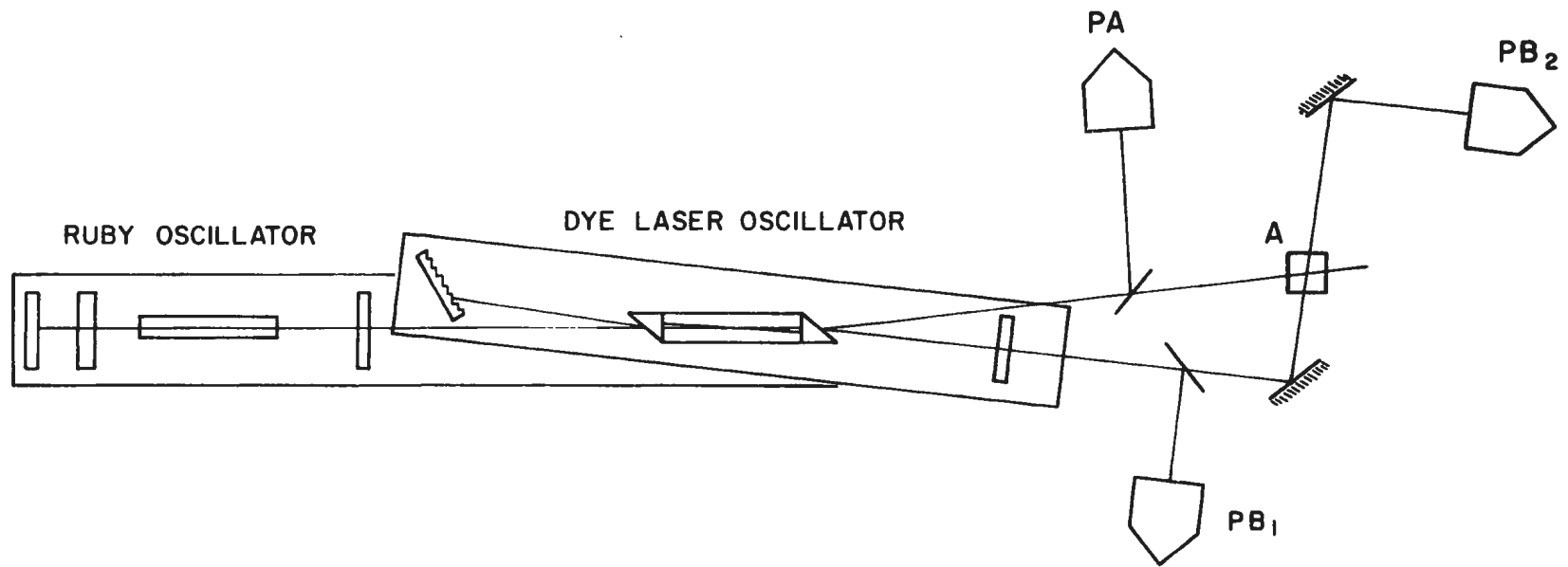


Figure 1. Experimental setup used for gain measurement

The laser cavity was formed by two plane reflectors; a dielectric coated quartz rear reflector with a reflectivity greater than 99% at the ruby laser wavelength, and a sapphire disc front reflector without reflective coating. Both reflectors were flat to within 1/10 wavelength at  $6943 \text{ \AA}$  and the surfaces were parallel to within 2-4 seconds of arc.

Polarization of the laser pulse was controlled through orientation of the laser rod. In the present case, the "C" plane of the ruby was made horizontal, giving a plane polarized laser output whose electric field vector is vertical.

The total energy in each laser pulse was measured by a TRG Model 100 thermopile with a sensitivity of  $240 \text{ \mu V/joule}$ . An ITT biplanar vacuum photodiode with an S-1 response, in conjunction with a Tektronix Model 519 oscilloscope with a rise time of 0.3 ns, was used to record the temporal profile of each laser pulse. A narrow band interference filter placed in front of the photodiode blocked all light except the ruby laser light.

#### Dye laser oscillator:

The dye laser oscillator was designed and constructed as part of the present research project. In Fig. 2, which shows a schematic diagram of the dye laser system in a longitudinal pumping configuration, the three main components of the dye laser are indicated. These are: (i) the dye cell, (ii) the rear reflector, and (iii) the output reflector. The longitudinal pumping configuration was used throughout the present investigation because of the smaller beam divergence characteristic of this arrangement and because with this arrangement longer dye cells of

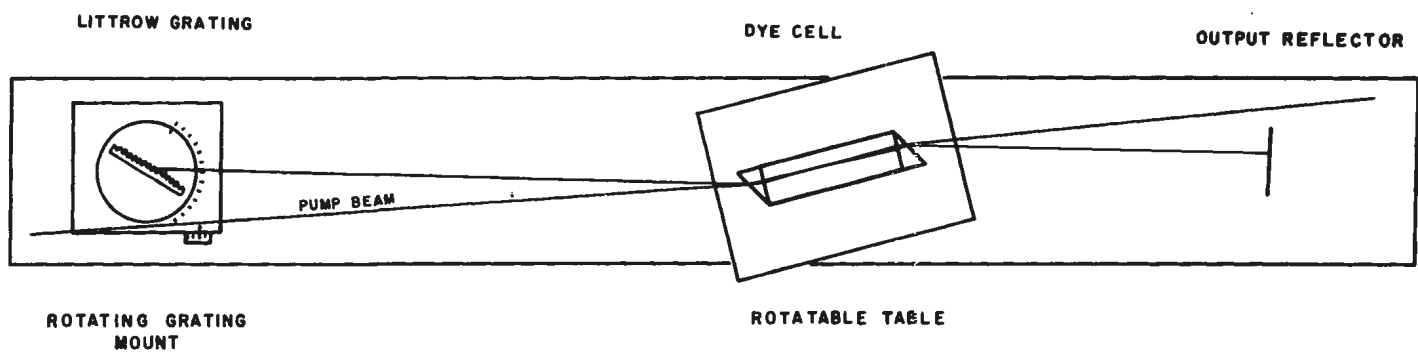


Figure 2. Dye laser oscillator

relatively simple construction could be used.

The dye cell was a cylindrical glass tube 8.0 cm in length and 0.5" in diameter, with Brewster prisms attached with RTV silicon rubber cement to the cell ends as windows. Orientation of this cell with its windows at the Brewster angle with respect to the axis of the laser cavity was accomplished by placing it on a rotatable table.

Two plane reflectors formed the optical cavity; the front reflector being a dielectric coated quartz disc 1" in diameter by 1/8" thick, flat to  $1/10 \lambda$ , with reflectivity of at least 65% from  $7000 \text{ \AA}$  -  $8500 \text{ \AA}$ , the rear reflector was either a 99% reflector with the same optical properties as the front reflector or a plane diffraction grating set in autocollimation. This grating had 2160 lines/mm and was blazed at  $5000 \text{ \AA}$  in the first order. It was mounted on a table designed specifically for this purpose, which could be rotated by turning a knob at its side. Table rotation was measured in degrees from the normal to the cavity axis by a dial at the side calibrated in units of 1/20th of a degree. The resolution of the dial setting was about 1/4 of one dial division or slightly better than 1 minute of arc and the resetability was about the same, corresponding to a wavelength variation of approximately  $1 \text{ \AA}$  at the peak wavelength of the laser emission.

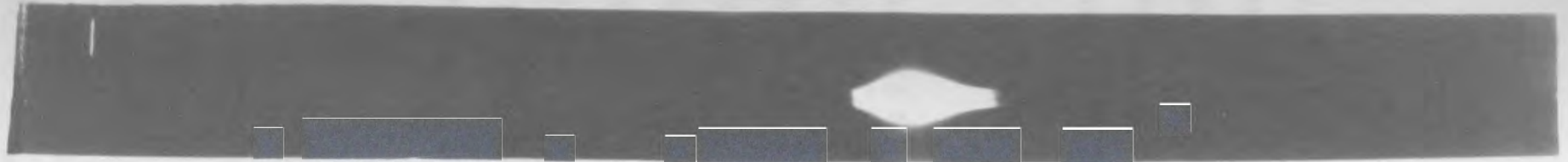
With this apparatus, several dyes each exhibiting laser action at different wavelengths were investigated for efficiency, output linewidth, and ease of use. Table 1 lists these dyes, their solvents and concentrations, and the wavelength region in which each dye lases. Fig. 3 shows broadband spectrograms of three of these dyes for the solvent and concentration listed in Table 1.

TABLE I

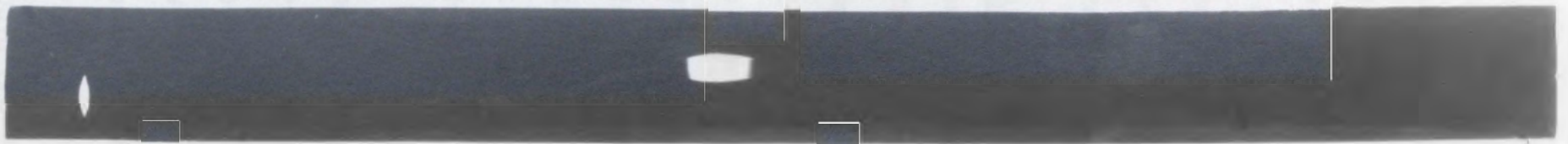
Dyes which showed laser action, and their spectral ranges

Dye	Concentration	Solvents	Wavelength range
3,3' diethyl thia- tricyanaine iodide	$10^{-5}$ M/l	methanol	7850 Å - 8400 Å
cryptocyanine	$10^{-5}$ M/l	glycerol	7250 Å - 7600 Å
1,1' diethyl-22' thia- dicarbocyanine iodide	$10^{-5}$ M/l	acetone	7050 Å - 7400 Å
1,1' diethyl-2,2'- tricyanaine iodide	$10^{-6}$ - $10^{-5}$ M/l	acetone	8600 Å - 9600 Å
1,1' diethyl-22' di- carbocyanine iodide	$10^{-5}$ M/l	glycerol	7150 Å - 7400 Å

(i) 3,3' diethylthiatricarbocyanine iodide



(ii) cryptocyanine



(iii) 1,1' diethyl-2,2' thiadicarbocyanine iodide



Neon standard



6328

6506

6678

6929

7032

7174

7245

7439

7544

8136

8301

8378

8495

8591

Figure 3. Spectrograms showing broadband laser output for three dyes

In the experiment to measure gain, only the dye DTTC, which lases in the region  $7800 \text{ \AA} - 8400 \text{ \AA}$  was shown. Tuned laser output spectra for this dye are shown in Fig. 4 where it is seen that at the expense of a small decrease in energy the spectral width of the laser is decreased by a factor of 100. A broadband spectrum is also shown in Fig. 4 and it should be noted that for a given concentration of dye the tunable range is greater than the broadband width.

#### B. Gain measurement:

Gain measurements were made with the experimental arrangement shown in Fig. 1. The sequence of events was as follows: A ruby laser pulse optically pumps the dye laser oscillator which then lases simultaneously with the ruby laser. The ruby laser light transmitted by the dye laser oscillator ( $\approx 20\%$ ) was used to transversely pump the amplifier cell, and a fraction of the dye laser pulse was used as a probe pulse to be amplified. Since the dye laser oscillator produced its maximum output at the same time as the ruby laser oscillator (experiments showed this to be true to within  $\sim 1 \text{ ns}$ ), synchronization of the probe pulse and the pumping pulse in the amplifier was achieved.

In order to measure the dependence of the gain on the intensity of the pumping beam, the ruby laser pulse was attenuated by placing a cell containing various concentrations of cobalt chloride in ethanol in its path. The intensity of the pumping beam was varied over a range of  $0.5 \text{ MW/cm}^2 - 7.0 \text{ MW/cm}^2$ . The intensity of the probe beam was attenuated by a solution of copper sulphate in water to yield intensities between  $1 \text{ KW/cm}^2$  and  $10 \text{ KW/cm}^2$ . This was the lowest probe beam intensity at the photodiode which would provide a half scale deflection on the oscilloscope.

Broadband DTTC



Tuned DTTC full range



Tuned DTTC single line



Neon standard



6328 —  
6506 —  
6678 —  
6929 —  
7032 —  
7174 —  
7245 —  
7439 —  
7544 —  
8136 —  
8301 —  
8378 —  
8495 —  
8591 —

Figure 4. Tuned laser spectra for DTTC dissolved in methanol ( $10^{-5}$  moles/liter)

A rectangular quartz container with dimensions 1 cm x 1 cm x 4.5 cm was used as the amplifier cell. Apertures were placed on the cell to control both pump and probe beam cross sections. For the pump beam, a 1 cm x 1 cm square aperture was used so that the pump light could illuminate the entire region through which the probe beam passed. For the probing beam, a circular diaphragm 9 mm in diameter was used.

The temporal profiles of the input pulse to the amplifier cell, and the amplified output pulse were monitored by photodiodes  $PB_1$  and  $PB_2$ , respectively (Fig. 1). Both of these photodiodes were connected to a single oscilloscope in such a way that the pulse from photodiode  $PB_2$  arrived at the oscilloscope 40 ns after the pulse from photodiode  $PB_1$ . The pumping pulse incident on the amplifier cell was recorded by photodiode PA of Fig. 1, in conjunction with another oscilloscope. Photodiode  $PB_2$  was set 50 cm from the amplifier cell in order to reduce the intensity of fluorescence from the amplifier cell incident on it. A diaphragm placed in front of this photodiode also helped. The amplifier cell itself was set so that the probe beam was not exactly normal to the surface but was offset about  $2^\circ$ . This was so that reflections from the surfaces of the amplifier cell could be blocked by the diaphragm in front of the photodiode.

#### Reduction of data:

The experimental data consisted of oscillograms of the output from three photodiodes connected to two Tektronix model 519 oscilloscopes. For each experimental run, or firing of the laser, one oscillogram showed the input (probe) pulse and the amplified output pulse from the

amplifier cell. The other oscillogram showed the pumping pulse. Each temporal pulse profile was then reduced to digital information by measuring the heights of the pulse trace at 2 ns intervals.

In order to compute the gain, the input and output photodiodes had to be calibrated with respect to each other. This was done by blocking the pumping beam and filling the amplifier cell with only the solvent for the dye. Then the output from the amplifier cell was evaluated as a function of the input to the amplifier cell. Thus, from a knowledge of the input to the cell, the output from the cell with no dye in the cell could be predicted. The relationship between the photodiode outputs was obtained by fitting a least-squares polynomial. Polynomials of up to fifth order were attempted, and in all cases the linear fit proved to be the best fit. Also, the polynomials obtained for each wavelength were within 5% of the average value, so it was decided to choose one representative curve for all the wavelengths used in the experiment. This straight line fitted the data remarkably well, as shown in Fig. 5. The equation for this straight-line fit was

$$P_{\text{out}} = (0.827 \pm 0.063) \times P_{\text{in}} - (0.019 \pm 0.025) \quad [2]$$

Since the constant term was small, and was in fact smaller than the magnitude of the error in the term, it was taken to be zero. It was expected to be zero anyway since, for no power input, one expects no power output.

This calibration equation was applied to single measurements, and the error in the result was taken to be the error in the measurement. Therefore, the constant term should represent the measurement error of a

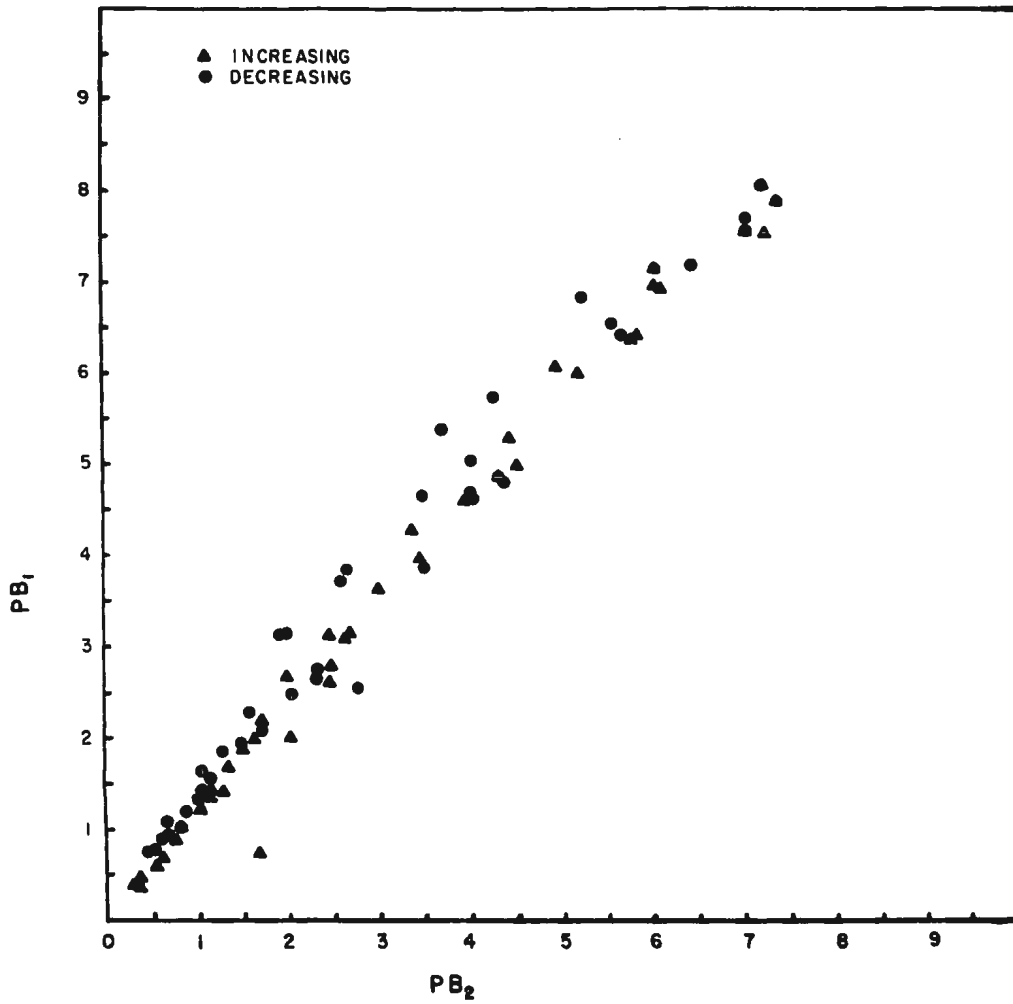


Figure 5. Relative photodiode calibration

single point, which was taken to be half the thickness of the line on the photographic trace, or 0.1 mm. This corresponds to four times the computed error standard deviations, so these were scaled by a factor of four in the subsequent analysis.

To see if there was any appreciable temporal distortion between the input and output probing pulses, a point-by-point comparison was made for several sets of typical input and output data taken when there was no dye in the amplifier cell. Fig. 6 shows typical sets of input and output pulses plotted together, whose maximum pulse heights were adjusted to give equal values. It can be seen that the shape of the pulses is preserved by the amplifier cell without dye.

The next step was to see whether or not there was any detectable difference in the rising and falling parts of the input and output probing pulses. This should indicate any hysteresis effects in the detecting system by showing a slightly different slope when the rising sides of the input and output probing beams are plotted against each other from that when the falling sides of the input and output probing beams are plotted against each other. As can be seen in Fig. 5, the two sets of points representing the rising and falling parts of the pulse lie reasonably well on one and the same line.

#### Absolute power calibration of photodiode PA:

The pumping power incident on the amplifier cell was measured on photodiode PA of Fig. 1. This photodiode was calibrated absolutely by measuring the total energy incident on an area of the size of the input face of the amplifier cell. The area under each oscilloscope trace was calculated by the trapezoidal rule for integration, using the

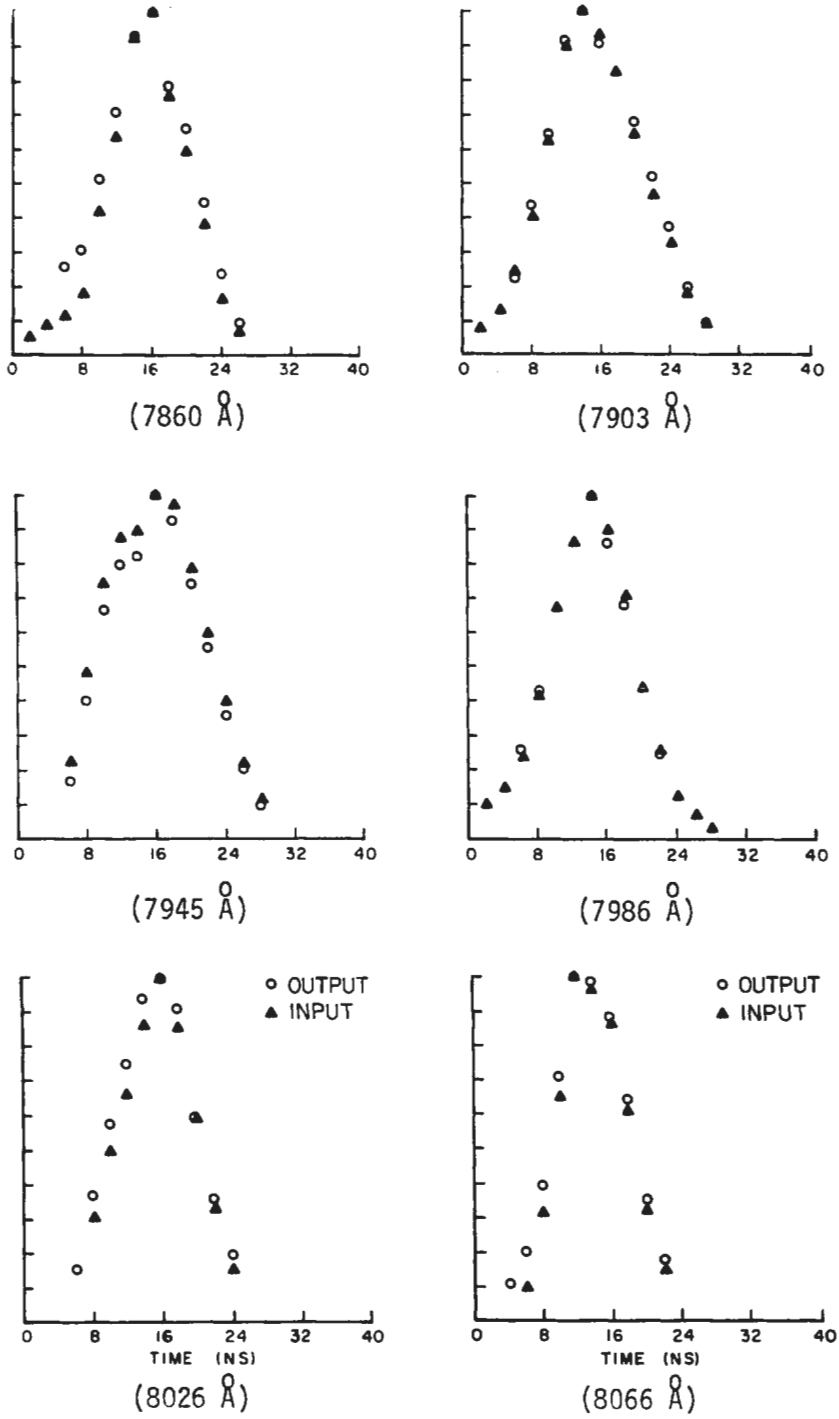


Figure 6. Normalized input and output pulses for each of the six wavelengths used in the gain experiment

measured pulse heights at 2 ns intervals. This area was set equal to the measured energy in the pulse. The energy delivered to the system in each 2 ns interval was then calculated from the ratio of the area under the pulse for this interval to the area under the entire pulse. The pump power, taken to be at the midpoint of this 2 ns interval, was then the energy in the interval divided by 2 ns. We have, therefore, that

$$P = (\text{Calibration}) \times \frac{(\text{area in 2 ns interval})}{2 \text{ ns}}, \text{ where}$$

$$\text{Calibration} = \frac{\text{total energy in pulse}}{\text{total area under pulse}} .$$

Such measurements were performed for a range of total pulse energies in order to see if the response of the photodiodes was linear. This is also shown in Fig. 7, where the absolute power calibration is plotted against the total energy in the pulse. If the photodiode response is linear, then this calibration should be constant. The results were scattered over a range of about 10% from the mean value, but this is reasonable since the oscilloscope error is  $\pm 3\%$ , the thermopile error is  $\pm 5\%$ , and the uncertainty in measurement of the area is about  $\pm 5\%$ .

In order to measure the gain with the amplifier full of dye, one records the output from the amplifier on photodiode  $PB_2$  of Fig. 1 and the input to the amplifier on photodiode  $PB_1$  of Fig. 1. From the calibration equation, the output, had there been no dye in the amplifier, could be predicted, and the gain is simply the ratio of the observed output to the input after applying the calibration equation. The gain coefficient  $G$  is the logarithm of this ratio or, in our case,

$$G = \log \left( \frac{I_{\text{out}}}{0.828 \times I_{\text{in}}} \right) .$$

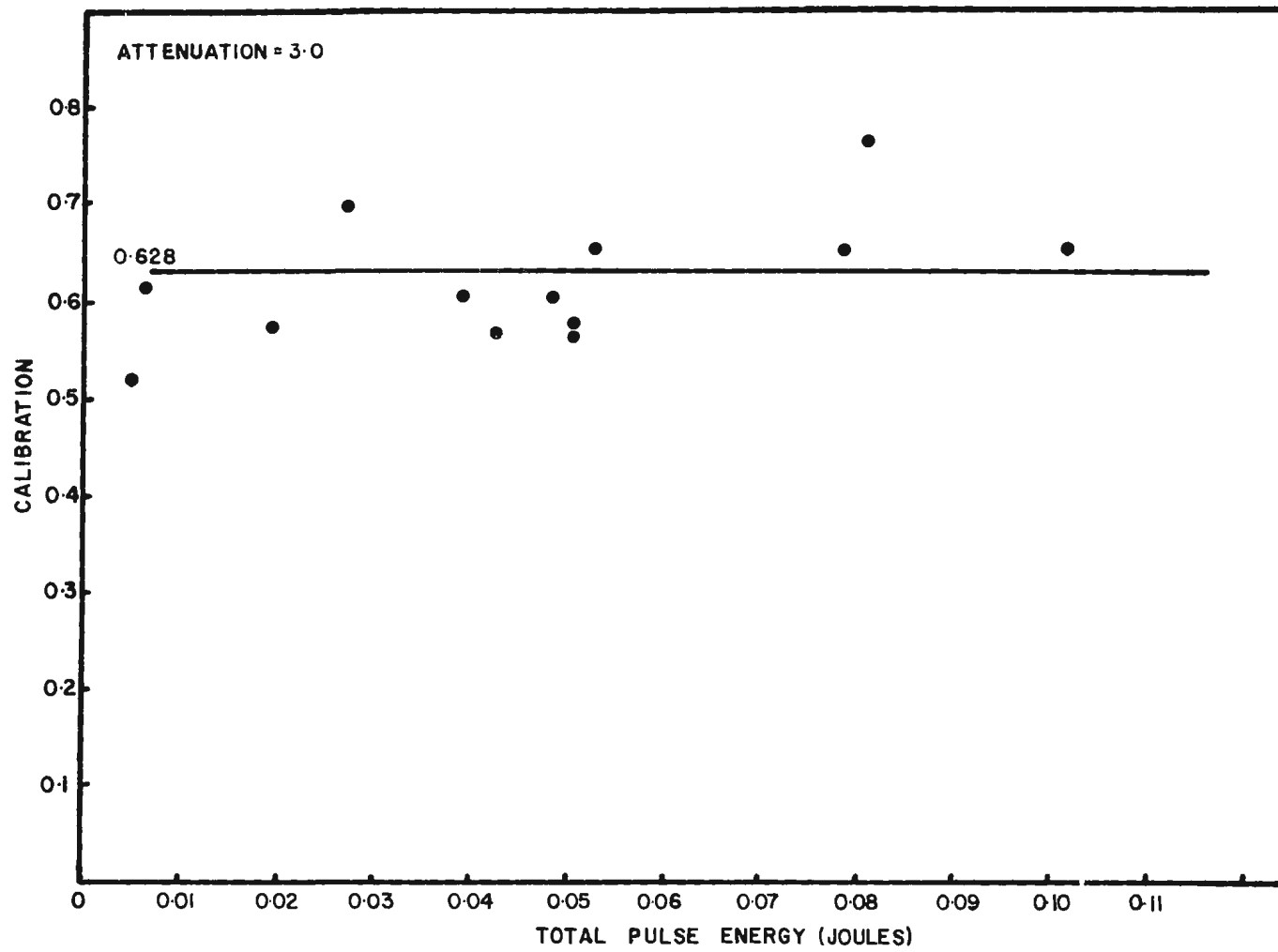


Figure 7. Absolute power calibration of photodiode PA of Figure 1

Temporal correlations:

First of all, an attempt was made to determine if the pumping and probing laser pulses arrive at the amplifier cell simultaneously. This was accomplished in the following two steps: First, the output from photodiodes PA and PB<sub>1</sub> of Fig. 1 were connected to the same oscilloscope; photodiode PA being connected through a delay cable of 40 ns and photodiode PB<sub>1</sub> connected directly. The output of the dye laser oscillator was then blocked before reaching photodiode PB<sub>1</sub> and a glass plate was placed in the path of the ruby laser beam to deflect part of it into photodiode PB<sub>1</sub>. The positions of the peaks of the two pulses on the oscillogram in this configuration of photodiodes were thus calibrated as the points of coincidence in time. Time differences in any pulses received by the two photodiodes PA and PB<sub>1</sub> could therefore be measured as relative shifts of the second peak with respect to the first. Secondly, the reflector in the path of the ruby laser pulse was removed, and the output from the dye laser was allowed to reach photodiode PB<sub>1</sub>. The time difference between this light and the ruby laser light was then measured. It was found that the positions of the peaks of the pulses were in all cases coincident to within 1 ns. This uncertainty was well within the experimental error which could be introduced by difficulties in finding the true maxima of the pulses because of the flatness of some of the pulse peaks. In the gain experiment, these two pulses are on different oscillograms but, since their peaks correspond to the same point in time, the pulses could be related to one another point-by-point in time.

## CHAPTER 3

### RESULTS AND DISCUSSION

#### Analysis of data:

In order to calculate the gain, oscillograms for the pumping pulse, and input and output probing pulses were reduced to digital information by measuring the pulse heights at 2 ns intervals. Oscillograms were reduced in this manner for each of six dye laser wavelengths from 7860 Å to 8066 Å, and for various peak pumping powers. The input and output probing pulses were recorded on the same oscillogram and separated by 40 ns on the time scale by having the output pulse travel a length of cable with a delay time 40 ns greater than that travelled by the input pulse. Gains were therefore calculated by comparing the pulse heights with the corresponding pulse heights 40 ns later on the oscillogram. The gain was computed after an appropriate adjustment was applied to the input power  $P_{in}$  by means of the calibration equation (Eq. 2). The logarithm of the ratio  $\frac{P_{out}}{P_{in}}$ , output power to input power in  $MW/cm^2$ , after the above adjustment, was taken as the gain coefficient.

After the gain coefficient was calculated for each data point, it was analyzed as a function of pumping power, wavelength, and time. For each oscillogram, the input, output, and pumping pulses were plotted by the computer plotter, together with a plot of the gain of the dye against time.

Gain as a Function of Time:

Fig. 8 shows (i) plots of the gain against time for typical oscillograms, and (ii) profiles of the pump pulse, input pulse, and output pulse for the amplifier. The gain against time curves follow the general shape of the pumping pulse, but the trailing edge of the gain shows a slightly greater slope than the leading edge. This seems to imply that time is not a very significant factor in the gain, but that there is nevertheless some time dependent effect for points on the trailing side of the pump pulse.

In order to further investigate the degree of time dependence in the gain, the gain data in the range 3 MW - 7 MW was fitted to polynomials of up to third order in pumping power and time measured from the beginning of the pulse. In no case was the dependence of the gain on time as great as the probable error in the pumping power measurements, which indicates that effects due to the explicit parameter time are less than the experimental error of about 10%.

The gain was also analyzed in a similar manner as a function of the instantaneous pumping power in the range 3 MW - 7 MW and the cumulative pump pulse energy up to that instant. Again, the gain showed no significant dependence on pump energy. Therefore, it appears that the time and total energy effects are small compared to the uncertainty of the experiment, and their effects cannot be seen in the collective data. However, in individual measurements there sometimes appears to be some time dependent effect, possibly due to the population of some metastable state.

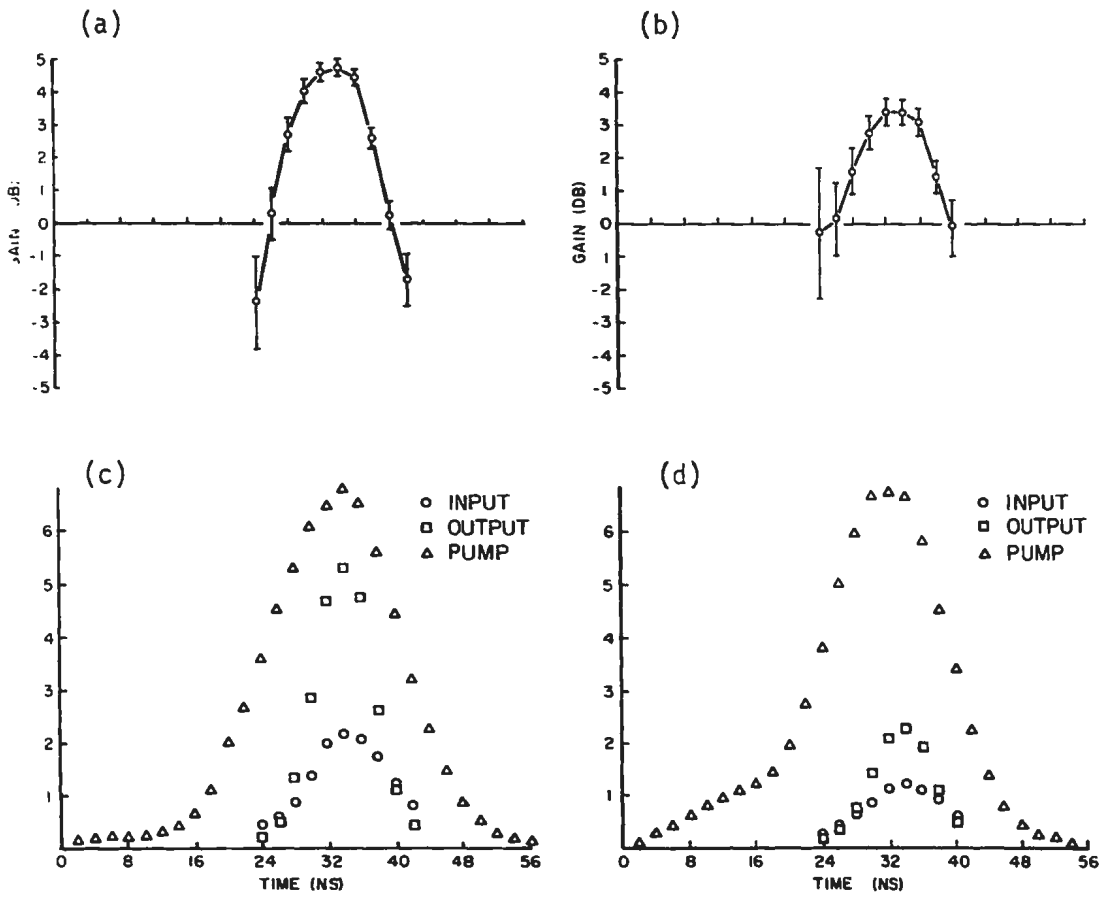


Figure 8. (a),(b) Gain as a function of pulse time; (c),(d), Profiles of the pump pulse and the input and output pulses to the amplifier cell

Gain as a Function of Instantaneous Pump Power:

As mentioned previously, it was observed that the peak of the pumping pulse and the peak of the probing pulse were coincident in time to within 1 ns. This information is sufficient to establish point by point correspondence between the oscillograms of the pumping and probing pulses.

Figures 9(a)-(f) show the gain versus instantaneous pumping power for six wavelengths - 7860 Å, 7903 Å, 7945 Å, 7986 Å, 8026 Å and 8066 Å. The data for each figure was obtained from several groups of oscillograms in order to have a full range of pumping powers from 0 MW - 7.0 MW.

The features of the curves in each of the figures 9(a)-(f) are similar. In each case, the gain is proportional to the instantaneous pump power in the low power region, with

$$G = -\alpha + \beta P$$

where  $\alpha \equiv$  absorption coefficient

$\beta \equiv$  gain/unit pump power

$P \equiv$  instantaneous pump power,

and becomes constant for high pump powers. For low pump powers,  $\beta$  is a constant and for high pump powers  $\beta$  is a function of the instantaneous pump power. In Appendix I it is shown that, for low intensity probing pulses, the gain is given by

$$G = \frac{(\sigma_e + \sigma_a)NW}{A_{eg} + W} - \alpha$$

where  $\sigma_e$  is the cross section for stimulated emission of the probe beam,  $\sigma_a$  is the cross section for absorption,  $\alpha = \sigma_a N$  is the absorption coefficient of low intensity light at the wavelength of the probe beam,  $A_{eg}$

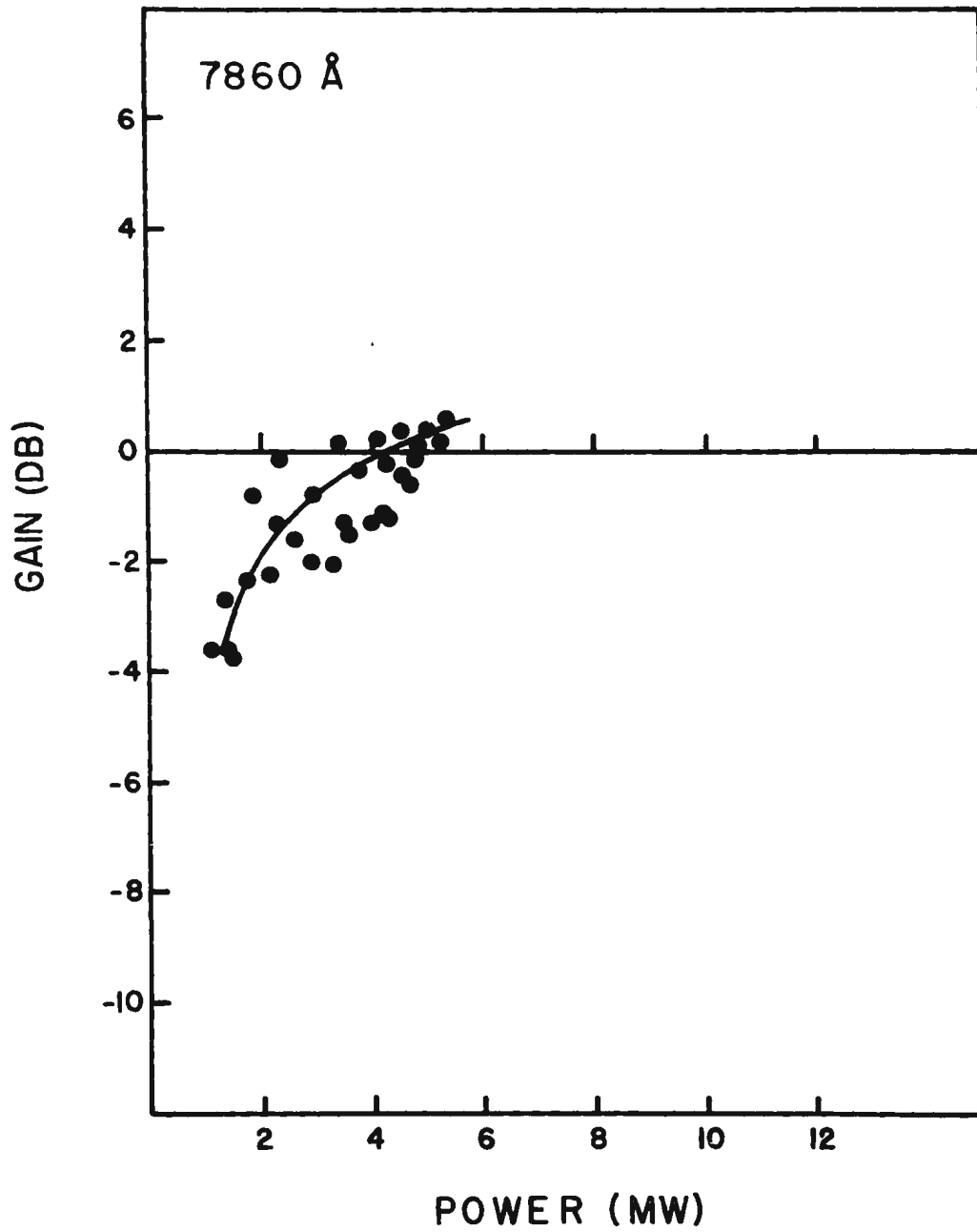


Figure 9. (a), Gain versus instantaneous pump power for wavelength  $\lambda = 7860 \text{ \AA}$

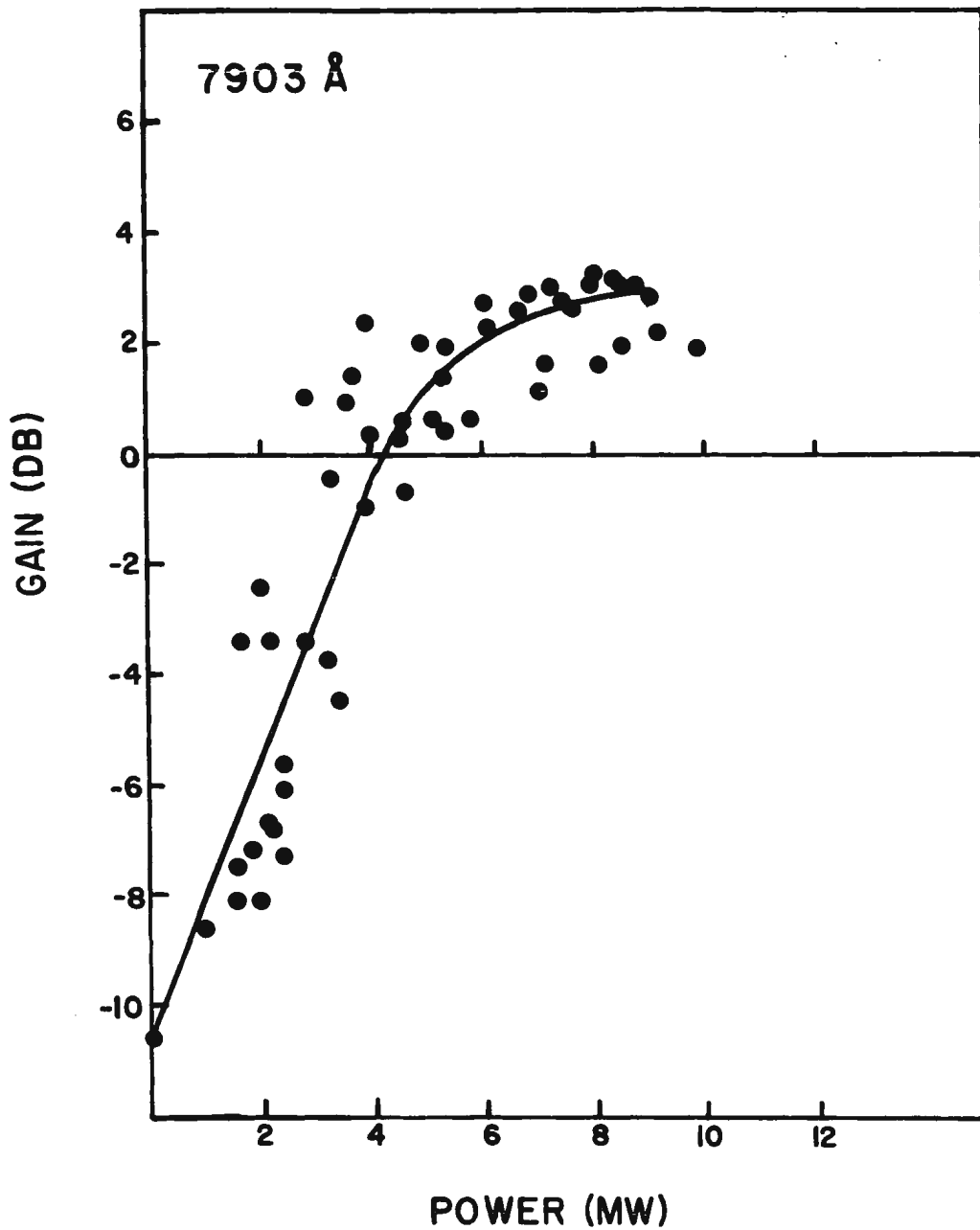


Figure 9. (b), Gain versus instantaneous pump power for wavelength  $\lambda = 7903 \text{ \AA}$

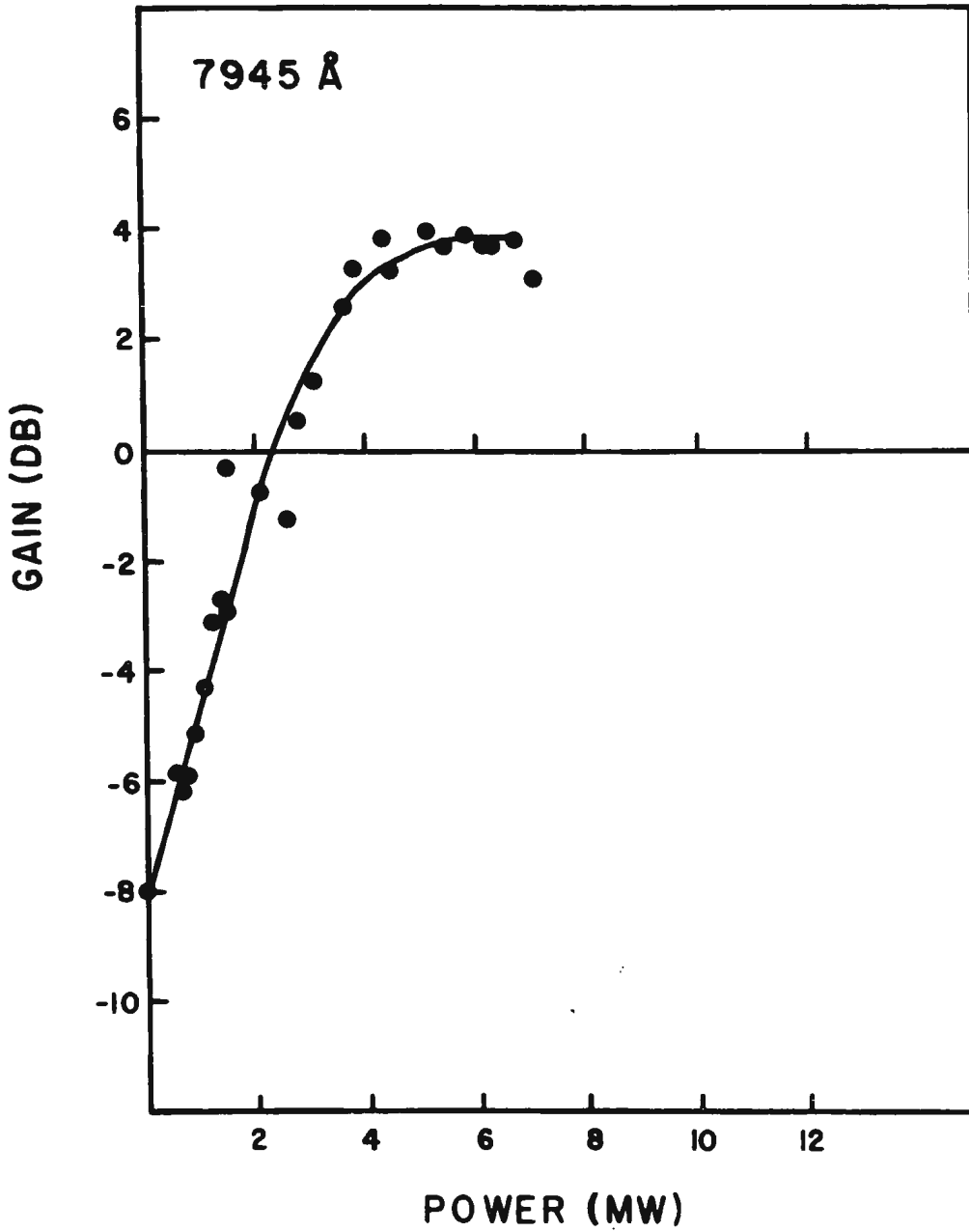


Figure 9. (c), Gain versus instantaneous pump power for wavelength  $\lambda = 7945 \text{ \AA}$

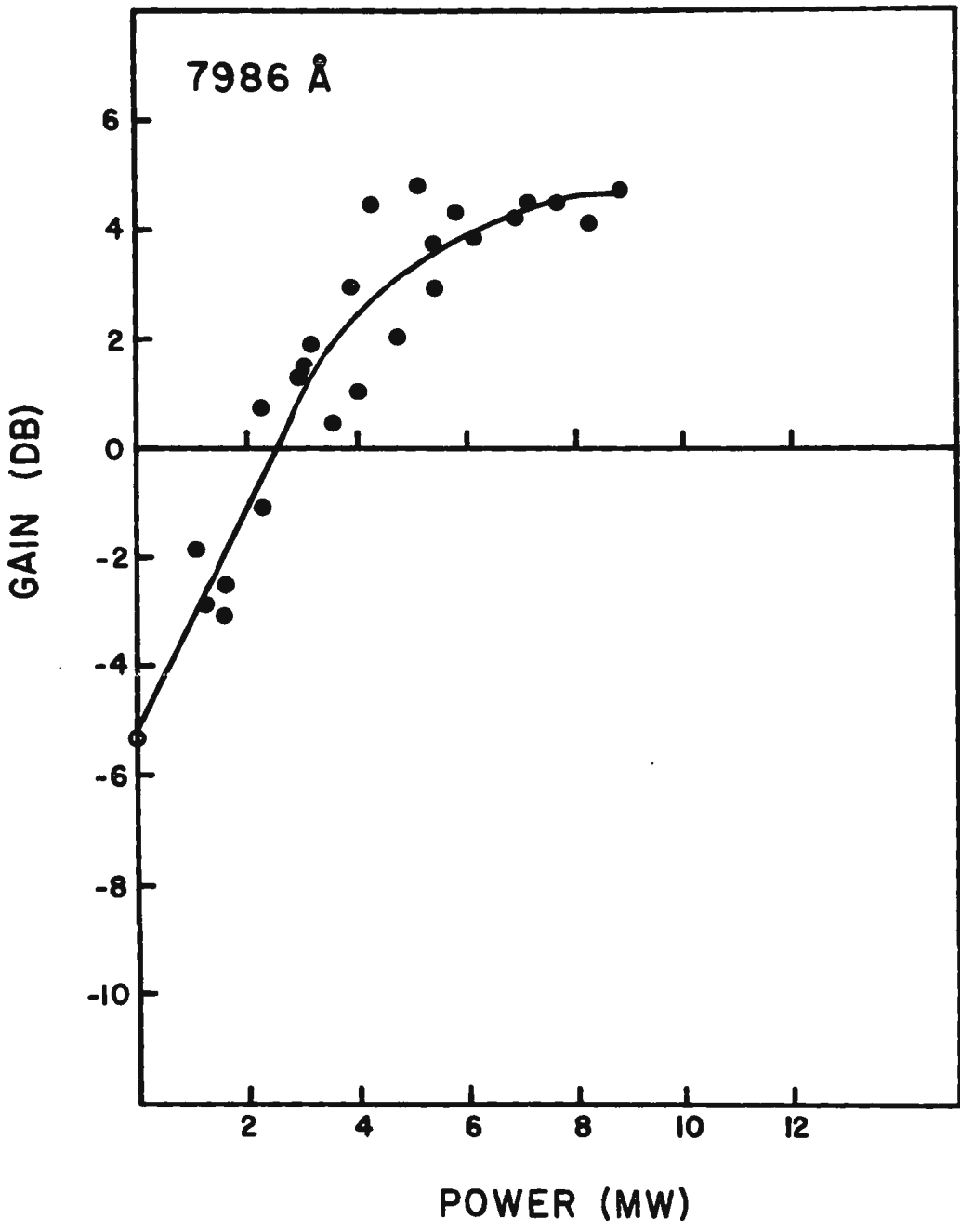


Figure 9. (d), Gain versus instantaneous pump power for wavelength  $\lambda = 7986 \text{ \AA}$

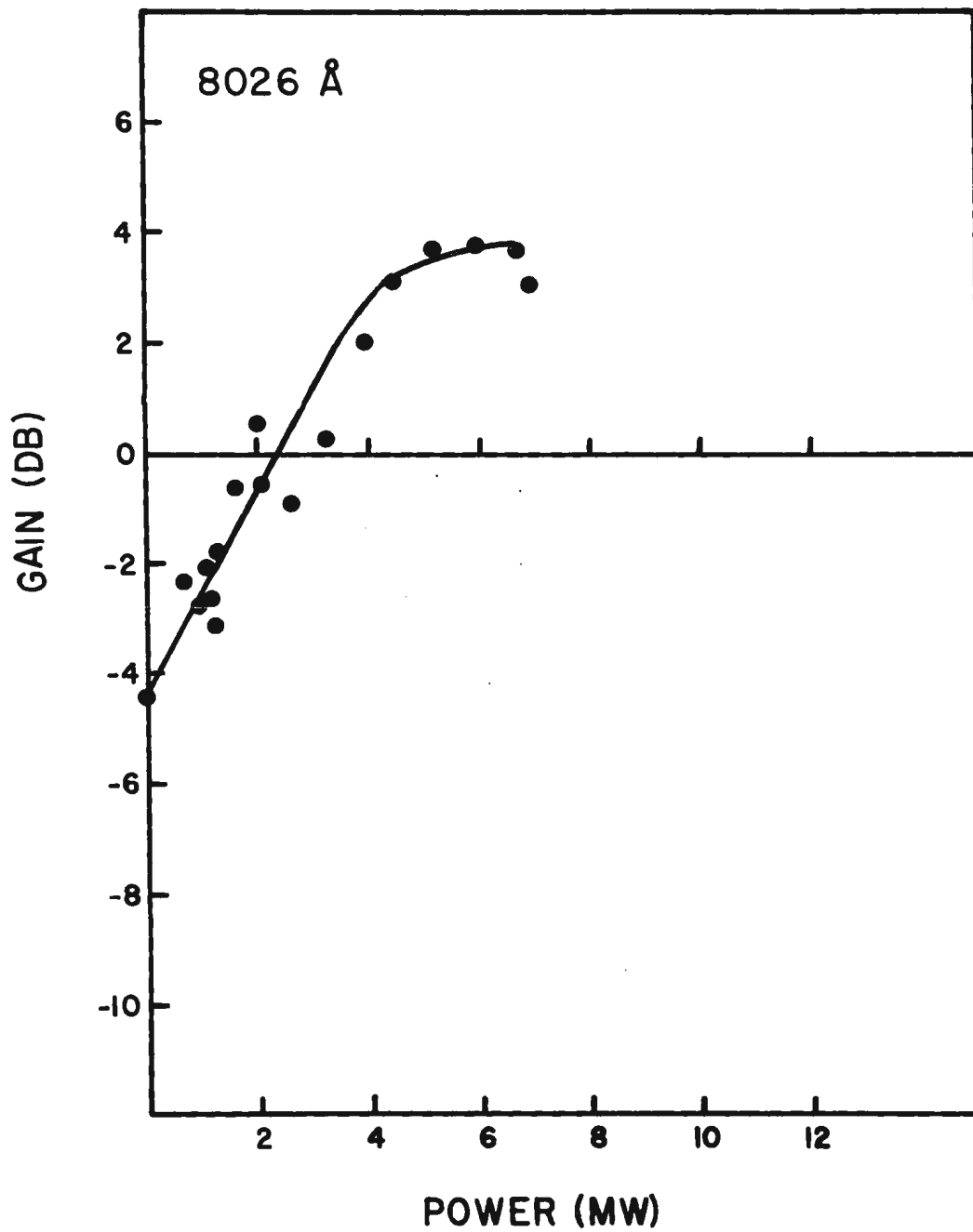


Figure 9. (e), Gain versus instantaneous pump power for wavelength  $\lambda = 8026 \text{ \AA}$ .

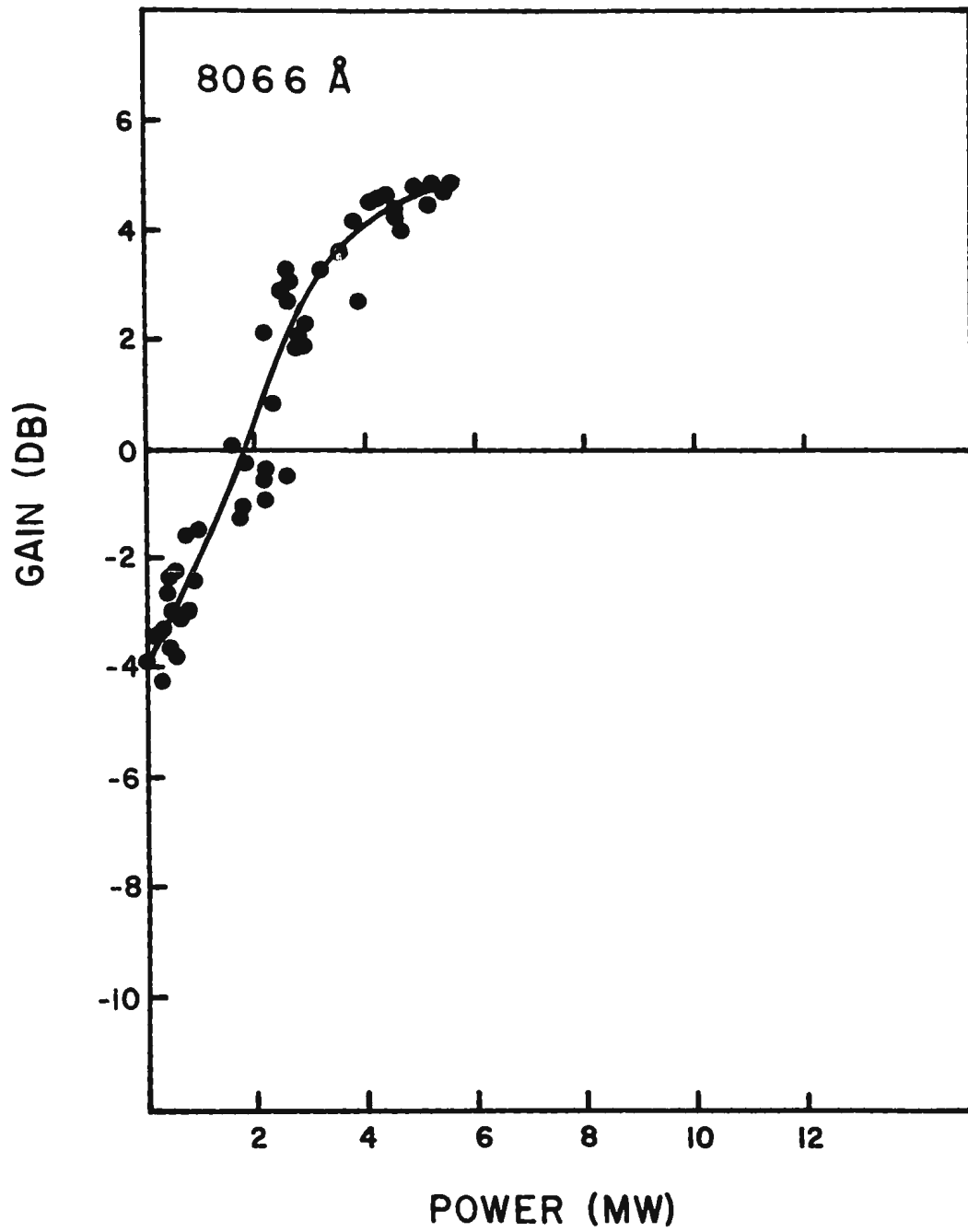


Figure 9. (f), Gain versus instantaneous pump power for wavelength  $\lambda = 8066 \text{ \AA}$ .

is the relaxation rate from the excited state to the ground state (including both radiative and nonradiative transitions), and  $W$  is the pump rate, or the rate at which ground state molecules are excited.  $N$  is the total number of molecules, and  $N_e$  is the number of molecules in the excited state.

It can be seen from Table II that the low signal gain coefficient  $\beta$  is maximum at  $7945 \text{ \AA}$ . This agrees with the results of Sorokin et al (4) who found the maximum broadband laser emission for DTTC dissolved in methanol to be  $7960 \pm 20 \text{ \AA}$ . The maximum value attained by the gain is at  $7986 \text{ \AA}$ , which coincides with the peak of the fluorescence spectrum reported by Sorokin et al (4).

It was not possible to measure the parameter  $W$  accurately as a function of pump power when the experiment was carried out, but subsequent measurements indicate that  $W$  does not vary by more than a factor of 3 in the range 0 - 10 MW. At low pump intensities,  $W$  is directly proportional to the pump power, so the term  $\beta$  can be identified with  $\frac{(\sigma_e + \sigma_a)N}{A_{eg}}$ , which is the slope of the lowest part of the curves in Figures 9(a)-(f). The upper limit of the function  $G$  (for high pump power) gives  $\sigma_e N$  directly, since for large  $W$ ,

$$G = (\sigma_e + \sigma_a)N - \sigma_a N = \sigma_e N \quad .$$

We can therefore find the stimulated emission cross section and the lifetime of the laser transition from the plots of gain against pump power. These results, together with the low pump power gain coefficient  $\beta$  and the absorption coefficient  $\alpha$  are given in Table II. Because the pump function  $W$  is uncertain, and since the result was derived from consideration of a two-level system, the result for  $A_{eg}$  should be considered correct only as to its order of magnitude.

TABLE II

Observed gain and attenuation constants for DTTC dye in methanol at various wavelengths,  
with the transition probabilities and cross sections for these wavelengths

Wavelength (Å)	Small signal gain coefficient (dB.cm/MW)	Absorption coefficient $\alpha_a$ (dB)	$\alpha_e = \sigma_e N$ (dB)	Stimulated emission cross section $\sigma_e (x 10^{17})$ (cm <sup>-2</sup> )	Spontaneous decay rate $A_{eg} (x 10^9)$ (sec <sup>-1</sup> )
7860 ± 5	—	—	0.8 ± 0.5	0.76 ± 0.54	—
7903 ± 5	2.0 ± 0.4	10.62 ± 0.53	3.6 ± 0.8	3.4 ± 1.2	7.9
7945 ± 5	3.2 ± 0.4	7.96 ± 0.56	3.9 ± 0.4	3.7 ± 1.1	5.6
7986 ± 5	2.4 ± 0.3	5.33 ± 0.41	4.7 ± 0.5	4.3 ± 1.3	6.8
8026 ± 5	2.04 ± 0.4	4.39 ± 0.73	3.9 ± 0.4	3.6 ± 1.1	6.5
8066 ± 5	2.3 ± 0.6	3.9 ± 0.6	4.8 ± 0.6	4.6 ± 1.3	3.7

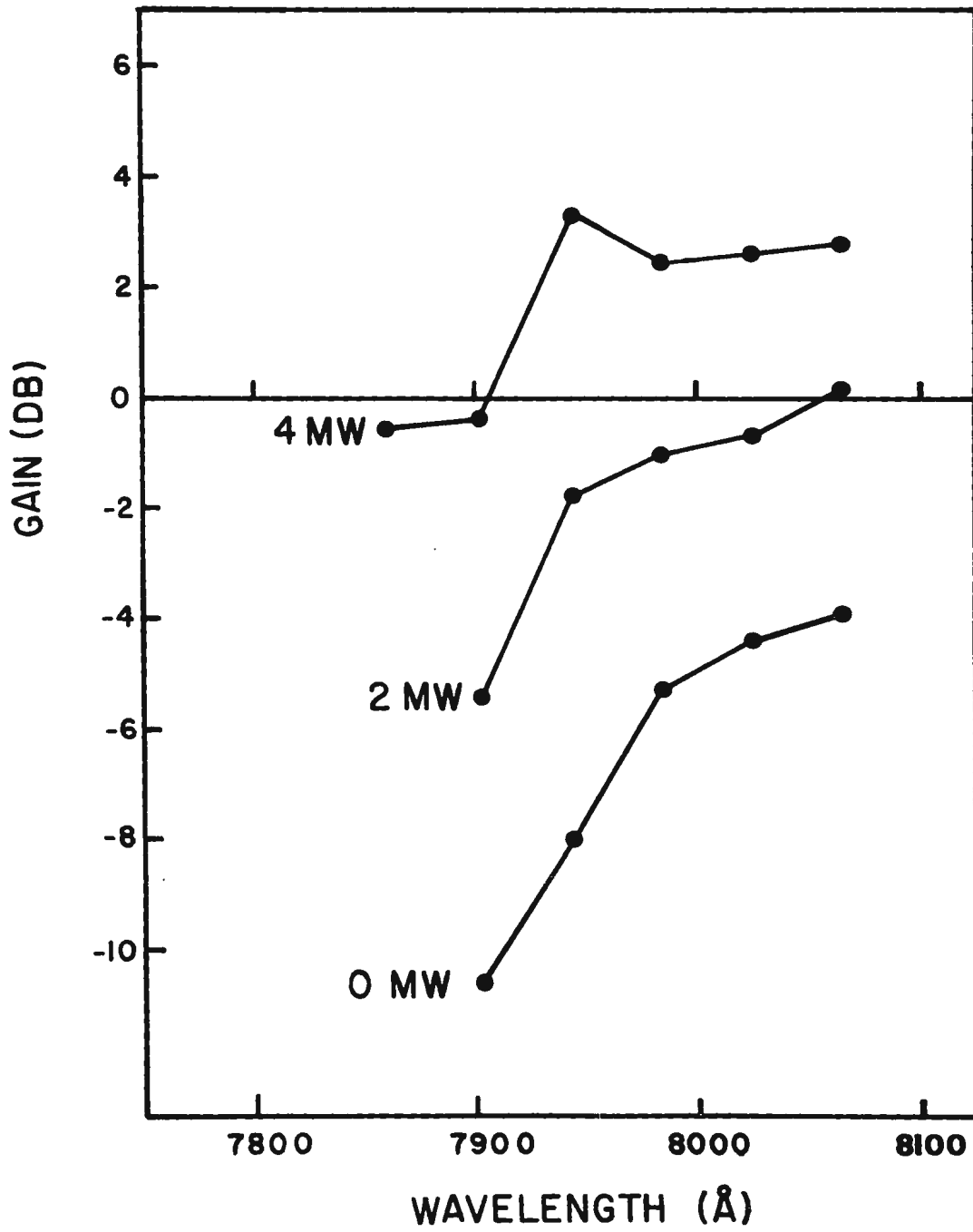


Figure 10. Gain versus wavelength for constant instantaneous pump power

The data points in Figures 9(a)-(f) represent gain measurements for instantaneous pump powers corresponding to the rising portion of the pump pulse, to minimize effects due to population buildup in metastable states. If gain is plotted for the rising and falling sides of pump pulses in the high power region, the gain is sometimes a double-valued function of the instantaneous pump powers with the gain for the falling side of the pulse being the smaller. An attempt was made to find possible explanations for this effect. The absorption of the pumping beam was measured as a function of pulse time to see if there was any significant change in the absorption coefficients in the amplifier during the pump pulse. These measurements were made under the same conditions as the gain experiment. The absorption was found to vary linearly with the input power for both the rising and falling side of the pulse, from  $\alpha = 10$  dB at low intensities to  $\alpha = 5$  dB at the highest intensities used. No strong effect due to the total energy absorbed was seen, and any changes in the absorption of pump light were too small to explain the double values for the gain as a function of instantaneous power. The observed effect is most probably due to (i) a buildup of excited molecules in some metastable triplet state making the pump energy unavailable, and (ii) reabsorption of the probe beam.

#### Gain as a Function of Wavelength:

Figure 10 shows the gain versus wavelength of the probe beam, as well as the zero pump gain, or absorption. It is seen that initially as the wavelength increases, the gain increases. This is due to the decrease in the low intensity absorption coefficient  $\alpha$ , and may possibly be enhanced by reabsorption of shorter wavelength emission. The curves indicate a

maximum in  $\beta$  at about 7950 Å which agrees with the centre of stimulated emission from a broadband DTTC-methanol dye laser as reported by Sorokin et al (4).

### CONCLUSION

Gain measurements as a function of pumping power and time have been made for the wavelength range 7850 Å - 8100 Å for a  $4 \times 10^{-5}$  M solution of DTTC dissolved in methanol. The gain was plotted as a function of pump power for each wavelength investigated (Fig. 9(a)-(f)). The low signal gain coefficient,  $\beta$ , was seen to be maximum at 7945 Å (Table II). This is consistent with the results of Sorokin et al (4) who reported maximum broadband laser emission for this dye in methanol at  $7960 \pm 20$  Å.

Theoretical expressions for the gain in two level amplifier systems were derived and from these and the measured data the stimulated emission cross section  $\sigma_e$  and the spontaneous decay rate to the ground state were evaluated for the dye at the measured wavelengths. The maximum in the stimulated emission cross section  $\sigma_e$  observed at 7986 Å coincides with the peak of the fluorescence spectrum as reported by Sorokin et al (4) at  $7985 \pm 30$  Å.

REFERENCES

1. A. L. Schawlow, C. H. Townes, Phys. Rev., Vol. 112, p. 1940 (1958)
2. E. G. Brock, P. Csavinszky, E. Hormato, H. C. Neddermann, D. Stirpe,  
F. Unterleitner, J. Chem. Phys., Vol. 35, p. 759 (1961)
3. S. I. Rautian, I. I. Sobel'man, Opt. Spectros. (USSR), Vol. 10, p. 134  
(1961)
4. P. P. Sorokin, J. R. Lankard, E. C. Hammond, V. L. Moruzzi, IBM J. Res.  
Dev., Vol. 11, p. 130 (1967)
5. A. Lempicki, H. Samuelson, Phys. Ltrs., Vol. 4, p. 133 (1963)
6. Y. Miyazoe, M. Maeda, Appl. Phys. Ltrs., Vol. 12, p. 206 (1968)
7. B. H. Soffer, B. B. McFarland, Appl. Phys. Ltrs., Vol. 10, p. 266 (1970)
8. D. J. Bradley, A. J. F. Durant, G. M. Gale, M. Moore, P. D. Smith,  
IEEE J. Quantum Electronics, Vol. QE-4, p. 707 (1968)
9. B. G. Huth, Appl. Phys. Ltrs., Vol. 16, p. 185 (1970)
10. C. V. Shank, A. Dienes, W. R. Silfvast, Appl. Phys. Ltrs., Vol. 17,  
p. 307 (1970)

APPENDIX I

The rate equations for a two level system, or a three level system where singlet-triplet transitions are not important, are

$$\frac{dN_e}{dt} = -\sigma_e N_e I - A_{eg} N_e + W(N - N_e)$$

where  $I = I(z,t)$  is the probe beam intensity

$\sigma_e$  is the stimulated emission cross section

$W = W(z,t)$  is the pump rate, or rate at which ground state molecules are excited

$N$  is the total number of molecules

$N_e$  is the number of molecules in the excited state.

The probing pulse  $I$  builds up in the amplifier as

$$\begin{aligned} \frac{dI}{dz} &= \sigma_e N_e I - \sigma_a (N - N_e) I \\ &= (\sigma_e + \sigma_a) N_e I - \sigma_a N I \\ &= (\sigma_e + \sigma_a) N_e I - \alpha I \end{aligned}$$

where  $\sigma_a$  is the cross section for absorption of the probe beam, and  $\alpha$  is the low intensity coefficient for absorption at the wavelength of the probe beam.

In the steady state,  $\frac{dN_e}{dt} = 0$ , so

$$N_e = \frac{WN}{\sigma_e I + A_{eg} + W} .$$

In general,

$$N_e = \left[ N_e^0 + \int^t NW \exp \left\{ \int^t (\sigma_e I + A_{eg} + W) dt' \right\} dt \right] \times \exp \left\{ - \int^t (\sigma_e I + A_{eg} + W) dt \right\} .$$

In the case of weak probe pulses,

$$\frac{dN_e}{dt} = - A_{eg} N_e + W(N - N_e) .$$

Therefore, at steady state,

$$N_e = \frac{WN}{A_{eg} + W} .$$

Now,

$$\begin{aligned} \frac{dI}{dz} &= (\sigma_e + \sigma_a) N_e I - \alpha I \\ &= \frac{(\sigma_e + \sigma_a) W N I}{A_{eg} + W} - \alpha I \end{aligned}$$

$$\frac{dI}{I} = \left[ \frac{(\sigma_e + \sigma_a) W N}{A_{eg} + W} - \alpha \right] dz$$

$$G = \ln \frac{I}{I_0} = \int_0^{\ell} \left[ \frac{(\sigma_e + \sigma_a) W N}{A_{eg} + W} - \alpha \right] dz .$$

If  $W \neq W(z)$ , as in the case of transverse pumping, then

$$G = \ln \frac{I}{I_0} = \left[ \frac{(\sigma_e + \sigma_a) N W}{A_{eg} + W} - \alpha \right] \ell .$$

This result is valid for transverse pumping as long as  $N_e$  does not depend on  $I$ ; i.e. as long as the probing pulse is very weak compared with the pumping pulse so that its presence does not alter the ground state

population. Also, the duration of the pumping and probing pulses must be long compared with the lifetime of the excited state ( $1/A_{eg}$ ) and short compared with the lifetimes of other mechanisms which deplete the excited state; e.g. singlet-triplet intersystem crossing. In these experiments there may have been small effects due to intersystem crossing, but their lifetimes are characteristically about  $10^{-7}$  sec in these dye materials, while the pulse durations in these experiments were less than  $3 \times 10^{-8}$  sec, so the singlet-triplet rate of intersystem crossing should not significantly affect the analysis.

#### ACKNOWLEDGEMENTS

The author wishes to acknowledge with thanks the following people, without whose assistance this project would never have been completed:

Dr. N. D. Foltz, my director, for suggesting the research problem and continued guidance throughout;

Dr. S. W. Breckon for continued interest and support;

Dr. C. W. Cho for many interesting discussions of the work;

Dr. A. O. Creaser for stimulating discussions of the theory;

Mr. C. T. W. Hsieh for assistance in taking measurements.

Messrs. Terry White and Adrian Walsh for the construction of most of the dye laser components.

Messrs. D. Seymour and G. Howcroft for constructing the dye cells and other glassware;

Dr. J. F. Ogilvie of the Chemistry Department for the use of a Unicam S.P. 8000 ultraviolet spectrophotometer, and other equipment;

Mr. Russ Tucker for assistance with the drawings for the thesis;

Mr. Ralph Alexander for the photographs in the thesis;

Miss Deanna Janes for typing the thesis.

